

# Kinetics of Visual Field Loss in Usher Syndrome Type II

Alessandro Iannaccone,<sup>1</sup> Stephen B. Kritchevsky,<sup>2</sup> Maria Laura Ciccarelli,<sup>3</sup> Salvatore A. Tedesco,<sup>4</sup> Claudio Macaluso,<sup>4</sup> William J. Kimberling,<sup>5</sup> and Grant W. Somes<sup>2</sup>

**PURPOSE.** To characterize the kinetics of visual field decay in Usher syndrome type II.

**METHODS.** The area of 137 Goldmann visual fields (GVFs) delimited with the I4e and V4e targets was measured in each eye of 19 patients with an established diagnosis of Usher syndrome type II, and the average interocular GVF area for each patient at each time point was calculated. The average follow-up was 5.58 years. Symptomatic disease duration was defined as years elapsed after symptoms were first noted. The data set ( $n = 67$  for the I4e target;  $n = 70$  for the V4e target) was analyzed with a random coefficient mixed model to identify the best-fit model describing the decay of visual field size over time. The half-life of the residual visual field area ( $t_{0.5}$ ) was also calculated.

**RESULTS.** The variable that best explained the decay of the GVF area was the duration of symptomatic disease. In an exponential model, the slope estimate for the natural log of the GVF area was  $-0.172$  for the I4e target and  $-0.136$  for the V4e target for each year of symptomatic disease. Accordingly,  $t_{0.5}$  was approximately 4 years for the I4e target and 5 years for the V4e target. These estimates are very similar to those in previous studies of nonsyndromic retinitis pigmentosa (RP).

**CONCLUSIONS.** This study suggests that the kinetics of GVF decline in Usher syndrome type II are, on average, very similar to other forms of RP and that, once the disease becomes symptomatic, GVF deterioration follows stereotyped kinetics, even in patients with late-onset retinal disease. (*Invest Ophthalmol Vis Sci.* 2004;45:784–792) DOI:10.1167/iovs.03-0906

Hereditary retinal degenerations are a genetically and clinically heterogeneous group of diseases, sharing the common characteristic of leading to progressive degeneration of the retinal tissue due to an inheritable cause. The most common of these diseases is retinitis pigmentosa (RP), which is estimated to affect approximately 1 in 3500 people world-

wide.<sup>1</sup> Typically, RP leads to the development of night blindness and loss of peripheral vision. Ultimately, the most aggressive forms of RP can lead to widespread retinal degeneration and legal blindness.

RP is also associated with extraocular manifestations that define specific syndromes. One such condition is Usher syndrome, an autosomal recessive disorder characterized by retinal degeneration and congenital hearing loss. There are three main clinically recognized types of Usher syndrome, distinguished primarily on the basis of the type and severity of the compromise of the audiovestibular system.<sup>2–4</sup> Of these, Usher syndrome type II is characterized by mild to moderate hearing loss and preserved or minimally impaired vestibular function. Typically, neither hearing nor balance deteriorates over time in these patients. Progressive retinopathy, clinically indistinguishable from classic RP, typically develops in the childhood to adolescent years in all types of Usher syndrome.<sup>2,3</sup> However, instances of late-onset RP in molecularly validated cases of Usher syndrome type II have been reported.<sup>5</sup>

The natural history of RP has been the object of study for the past few decades. Several studies have characterized in detail the kinetics of visual field loss in RP.<sup>6–12</sup> The extrapolation of epidemiologic and natural history data from nonsyndromic RP to Usher syndrome requires caution, however. Nonsyndromic RP and Usher syndrome are genetically heterogeneous. With the exception of a specific *USH2A* mutation,<sup>13</sup> no change in any of the Usher genes has been implicated thus far as a cause of RP without hearing loss. It is presently unknown whether disease mechanisms and dynamics of Usher syndrome are the same as those underlying nonsyndromic RP. For example, it has been noted that in most patients with Bardet-Biedl syndrome, which is also genetically distinct from nonsyndromic RP, ERGs are nonrecordable, even when good visual field expanses can be documented.<sup>14</sup> This is in sharp contrast with typical nonsyndromic RP, in which full-field ERG amplitude and visual field area are closely correlated.<sup>15,16</sup>

There are numerous reports on the ophthalmic and extraocular manifestations of Usher syndrome. Among these, studies by life-table and logistic regression analysis have shown that patients with Usher syndrome type II are less likely to have macular atrophic changes, visual acuity less than 20/40, and smaller visual field areas with both small and large targets than are type I patients.<sup>17–19</sup> These cross-sectional investigations of Usher syndrome help us to better appreciate the range of disease expression and the greater severity of retinopathy in Usher syndrome type I compared with type II. However, to the best of our knowledge, there is no published longitudinal natural history study of visual function in patients of any age with Usher syndrome patients, nor has any study been undertaken to investigate the behavior of visual fields over time in patients with Usher syndrome.

The evaluation of patients with hereditary retinal degenerations is traditionally based on the combination of psychophysical and other objective measurements. The relative independence of the full-field flash electroretinogram (ERG) from patient performance makes it the most objective of the measurements and, as such, an excellent outcome measure for the assessment of retinal function in both natural history studies

From the Departments of <sup>1</sup>Ophthalmology and <sup>2</sup>Preventive Medicine, University of Tennessee Health Science Center, Memphis, Tennessee; the <sup>3</sup>Division of Ophthalmology, Fatebenefratelli Hospital, Isola Tiberina, Rome, Italy; the <sup>4</sup>Department of Ophthalmology, Università degli Studi di Parma, Parma, Italy; and the <sup>5</sup>Boys Town National Research Hospital, Omaha, Nebraska.

Supported by National Eye Institute Grant EY000409, Fight for Sight Grant GA99056, National Institute of Deafness and other Communications Disorders (subcontract to Program Project Grant DC01813); and an unrestricted grant to the University of Tennessee Health Science Center Ophthalmology from Research to Prevent Blindness, Inc. AI is the recipient of a RPB Career Development Award.

Submitted for publication August 19, 2003; revised November 22, 2003; accepted December 1, 2003.

Disclosure: **A. Iannaccone**, None; **S.B. Kritchevsky**, None; **M.L. Ciccarelli**, None; **S.A. Tedesco**, None; **C. Macaluso**, None; **W.J. Kimberling**, None; **G.W. Somes**, None

The publication costs of this article were defrayed in part by page charge payment. This article must therefore be marked "advertisement" in accordance with 18 U.S.C. §1734 solely to indicate this fact.

Corresponding author: Alessandro Iannaccone, Department of Ophthalmology, University of Tennessee Health Science Center, 956 Court Avenue, Suite D228, Memphis, TN 38163; iannacca@utm.edu.

and treatment trials.<sup>6,20</sup> However, the full-field flash ERG cannot provide information on the distribution of vision across the visual field. In addition, from a practical standpoint, it is the amount of residual visual field more so than the size of the ERG response that determines aspects of functional vision in the individual patient, such as the ability to move efficiently in the environment or drive.<sup>21</sup> Hence, there is great value in characterizing the behavior over time of a psychophysical measurement such as visual fields in patients with retinal degeneration, and especially in patients with Usher syndrome, whose hearing impairment limits their ability to use acoustic clues to improve their driving skills or other daily activities.

Therefore, we sought to characterize the kinetics of visual field decay in patients with Usher syndrome type II to gain a better understanding of the natural history of the retinal degeneration that affects these patients and how the kinetics and the rates of such decay compare with those thus far reported for nonsyndromic RP.

## MATERIALS AND METHODS

### Patient Population

**Inclusion and Exclusion Criteria.** Patients included in this study had an established diagnosis of Usher syndrome type II, with a typical rod  $\geq$  cone disease pattern (i.e., classic RP-like) of retinal degeneration by clinical, visual field, and ERG criteria,<sup>1-3</sup> and had a minimum of two reliable and complete Goldmann visual field (GVFs) tests obtained at least 1 year apart. A GVF was deemed to be reliable if the patient showed ability to fixate steadily during the test and consistency in detecting the location of targets on the perimetric chart. Test-retest reliability was assessed empirically on the basis of the reproducibility of the size and location of islands of vision and scotomatous areas compared with previous and, when available, subsequent tests. Serial GVFs were defined as complete if information for both the I4e and the V4e targets was available at two or more time points. Typically, these two targets were measured at each testing session. Therefore, repeated measurements of each target were available at the same time points for most of the subjects. If a target had been omitted at one follow-up testing session but had been obtained at the next one, a series of GVFs was still considered complete, and patients remained eligible for inclusion.

Any patient without the specific and certain diagnosis of Usher syndrome type II and without classic RP was ineligible to participate. This excluded from participation not only all patients with Usher syndrome type I or III, patients with hearing loss attributable to other causes, and patients with nonsyndromic RP, but also three cases of possible Usher syndrome type II but with a cone-rod pattern of retinal degeneration. This study adhered to the tenets of the Declaration of Helsinki and was approved by the Institutional Review Boards and/or Ethics Committees of the participating institutions.

**Ascertainment of Disease Status and Age of Onset of the Disease.** Disease status in the eligible participants was ascertained by clinical and functional diagnostic criteria—that is, presence of (1) retinal degeneration, as exemplified by evidence of loss of peripheral sensitivity to visual field testing with one or more targets and/or loss of ERG amplitude, with or without overt ophthalmoscopic evidence of pigmentary retinopathy; (2) “sloping,” nonprogressive sensorineural hearing loss by pure-tone audiometry criteria (i.e., affecting exclusively or primarily the high stimulation frequencies); (3) mild to moderate speech impediment (consistent with the congenital nature of the hearing loss); and (4) normal vestibular function.<sup>3</sup>

In addition, a series of standardized questions was posed to all patients at the time of first examination to characterize as accurately as possible the age of onset of the first symptoms of the retinal disease. The symptoms that were investigated were night blindness, visual field limitation, light aversion, and reduced visual acuity, despite the use of

correction. Based on this information, we calculated an estimate of symptomatic disease duration, which can be expressed as follows

Symptomatic disease duration

$$= (\text{age at examination}) - (\text{age of onset}) \quad (1)$$

After determining the duration of symptomatic disease, it was possible to normalize patients to a common zero point rather than characterize the disease stage by age, a criterion that does not take into account the inherent variability in age of onset, which in our cohort varied substantially (described later). The concept of duration of symptomatic disease herein proposed is similar to that of “years past critical age” proposed by Massof et al. in 1990.<sup>7</sup>

**Examined Cohort.** Thirty-two patients met the four aforementioned inclusion diagnostic criteria of Usher syndrome type II with a rod  $\geq$  cone pattern of dysfunction. Of these, disease was diagnosed in 27 by one of us (AD), the others by two other authors (CM, SAT) at the University of Parma. All patients reported night blindness as the symptom of onset of the disease. At the time of first examination, several patients were not yet aware of any limitation in their peripheral vision, and this lack of awareness was always associated with a relatively recent onset of night blindness as a presenting symptom.

Of these 32 patients who had an established diagnosis of Usher syndrome type II, 1 had to be excluded because only one visual field test result was available (lost to follow-up) and 11 because no visual field result was available at all (failed to return to complete the workup after initial clinical evaluation,  $n = 7$ ; unable to perform due to end-stage disease,  $n = 3$ ; too young to perform,  $n = 1$ ). Another patient with a small central island of vision, despite 20/20 vision, displayed erratic testing behavior, with multiple satellite islands of vision appearing and disappearing during serial testing in a completely inconsistent manner. For this reason, she was not considered a reliable participant and was excluded from the study.

All but one of our patients displayed minimal intra- and intertest variability and fairly consistent patterns of progression over time with all tested targets. One subject (patient [PT] 15), for whom only two serial observations were available and whose first visual field with the V4e target was only approximately 6° in radius, displayed a 45% improvement with the V4e target, whereas the field with the I4e target had mildly deteriorated at follow-up testing. Because spontaneous improvement<sup>6</sup> and test-retest variability of up to 48% in GVF size have been reported in RP,<sup>22</sup> especially with small visual fields such as those of PT15,<sup>9,23</sup> it was decided to maintain this patient’s data in the pool of analyzed data.

Once all these criteria were satisfied, 19 subjects remained eligible for inclusion in the investigation (Table 1). All participants were non-Hispanic whites; 11 were female. The duration of symptomatic disease spanned several decades in the patient sample. The age of onset of the first symptoms of the disease, which was night blindness in all cases, varied widely, with some patients symptomatic since childhood and others unaware of visual problems until the fifth decade of life (range, 5–42 years old). Two of the patients had visual field tests performed by an experienced examiner before first examination and testing by one of us. These visual fields met all criteria to be considered complete and reliable and were included in the analysis. Five patients contributed only two serial observations. All others contributed three or more observations—one as many as seven—spanning a follow-up period of up to 21 years. On the aggregate, 66 pairs of visual fields and five serial measurements obtained from the only eligible eye of one patient (PT10) were available for measurement from this cohort of 19 patients with Usher syndrome type II, for a total of 137 GVFs.

### Measurement of GVF Area

The isopters delimited with the standard I4e target and the V4e target represented the object of our investigation. After approximately 2 minutes of adaptation to the standard background light (31.5 asb) for each eye, GVFs were performed in all patients, by presenting the test

TABLE 1. Demographics, Clinical Information, and Basic Descriptive Statistics of the Patient Population Included in the Analysis

Patient Number	Sex (M/F)	Age at First Examination (y)	Age of Onset of Night Blindness (y)	Follow-up Years (n)	Serial Observations (n)
PT1	M	17	12	3	4
PT2	M	14	14	7	5
PT3	F	16	6	3	3
PT4	M	14	5	1	2
PT5	F	23	16	1	2
PT6	F	25	5	1	2
PT7	F	44	30	3	3
PT8	M	28	13	1	2
PT9	F	47	17	11	6*
PT10	F	52	25	7	5
PT11	F	51	42	3	4
PT12	M	51	20	4	3
PT13	M	40	6	9	5
PT14	F	22	18	3	3†
PT15	M	51	16.5	2	2
PT16	M	48	39	4	3
PT17	F	23	14	21	7‡
PT18	F	53	33	16	4
PT19	F	56	16	6	5
Average		35.53	18.29	5.58	3.68
SD		15.65	10.97	5.41	1.49
Median		40.00	16.00	3.00	3.00
Range		14–56	5–42	1–21	2–7

\* Five serial observations (obs.) for the I4e target.

† Two serial obs. for the V4e target.

‡ Four serial obs. for the I4e target.

targets with the customary, from not-seen to seen strategy for both peripheral isopters and scotomatous areas. Corrective trial lenses commensurate to refractive status and age of the patient were used only for GVFs of radius of 25° or less and only with the I4e target. When applicable, patients were allowed to keep contact lenses on throughout the test. Pupils were not dilated on any occasion. These methods were used consistently at each follow-up examination.

The average radius of the GVF was measured at 12 meridians (the main four meridians and eight equally spaced intermediate meridians, two in each quadrant) to obtain the estimated area, calculated simply as  $\pi r^2$  and expressed in square degrees ( $\text{deg}^2$ ). Any scotomatous area was measured with the same method and subtracted from the total area. This rapid and cost-effective method was very simple to implement and was quite accurate, comparing very favorably with software-based area estimations (0.999 coefficient of correlation with areas digitally measured with NIH Image, [ver. 1.63], on a sample of 30 representative fields from this cohort; NIH Image is available by ftp at [zippy.nimh.nih.gov/](http://zippy.nimh.nih.gov/) or at <http://rsb.info.nih.gov/nih-image/>; developed by Wayne Rasband, National Institutes of Health, Bethesda, MD). Because only PT18 had large ring scotomas at baseline with significant far peripheral islands of vision reaching temporally outside the central 55°, and all others with normal field expanses to V4e testing lost very little area with this target during the follow-up—thereby making these data points not influential on the final outcome of the statistical analyses (see the Results section)—no correction of the well-known perimetric cartographic errors that occur when transforming data from polar to planar coordinates was warranted in our cohort (see Ref. 24 for a complete discussion of this problem and review of the pertinent earlier literature).

As expected in all forms of typical RP,<sup>25</sup> visual field losses were symmetric between both eyes of our patients (interocular correlation coefficient: 0.994, results not shown). Therefore, once measured, the areas of both eyes were averaged, to obtain an interocular average of the visual field at each time point. This approach has been used before in studies of visual fields in RP.<sup>25</sup> The use of an interocular average was possible for all patients but one (PT10), whose vision in the left eye

was severely diminished by a complication (end-stage macular hole) that precluded her from having sufficient fixation in that eye to perform the visual field test. Therefore, in her case, only the measurements from the right eye were used. Targets other than the desired ones had been obtained on one occasion for V4e (target IV4e had been obtained instead in PT14) and on four occasions for I4e (target II4e had been measured instead on three occasions from PT17. No measure had been obtained on one occasion from PT9). Because of these missing measurements, analyses were conducted on 70 net serial data points for the V4e area and 67 for the I4e area.

## Statistical Methodology

All analyses were conducted on computer (SAS statistical software, ver. 8.1; SAS Institute, Inc., Cary, NC). GVF area data were analyzed both as raw values in square degrees and as natural log (ln)-transformed values, which approximated the normal distribution better. First, the area data for the I4e and V4e targets were plotted as a function of age and symptomatic disease duration, respectively, to observe the relationship between these two variables. After this, the area values were modeled statistically to determine which of the variables entered in our data set explained best the variation in visual field area over time. Because the data points within each subject correlated closely to one another (highly significant intraclass correlation coefficients, not shown), the data set required an analytic approach that would take into account this high within-subject correlation.

In our situation, it was reasonable to assume that regression coefficients (i.e., the intercept, or  $\alpha$ , and the slope of the function, or  $\beta$ ) were fixed effects—that is, unknown fixed parameters that are estimated from the data. Consequently, it was reasonable to assume that the regression model built on each pair of  $\alpha$  and  $\beta$  estimates for each subject would be a random deviation from the mean model of our study population. Therefore, the data set was analyzed by using a mixed model procedure. Specifically, because the data had a different number of repeated measures in each subject, we used a random-coefficient model-based method for the analysis.<sup>26</sup> This model does

not require the assumption of linearity of change in the dependent variables, takes into account the within-subject correlation of each subset of data points contributed by each subject, and attributes greater weight to subjects contributing more observations, as well as to those who fit the model best. This analysis method has been used before in previous natural history studies of GVF decay in patients with RP.<sup>7,9</sup>

The two dependent variable levels for which we tested the model were  $\ln(\text{area})$  I4e and  $\ln(\text{area})$  V4e. The main covariates that we evaluated in the model were age and symptomatic disease duration, the two criteria by which the areas of the visual field appeared to decline over time. We also evaluated the relationship of visual field area with baseline age and gender, either independently or together with the aforementioned temporal variables. In addition, to further characterize the kinetics of the decline of the visual field in Usher syndrome type II, we sought to determine the time constant ( $\tau_c$ ) of the decay of visual field area as a function of time. Because our analyses show that visual field area follows an exponential decay, the time constant was calculated as follows

$$\tau_c = -(1/\beta) \quad (2)$$

—that is, the negative reciprocal of the estimated slope ( $\beta$ ), as reported by Massof et al.<sup>7</sup> Furthermore, we used the estimated  $\tau_c$  in years to estimate the half-life ( $t_{0.5}$ ) of the visual field areas—that is, the amount of time (also in years) necessary for half of the remaining visual field area to be lost, which can be expressed as follows<sup>9</sup>

$$t_{0.5} = \ln(0.5) \cdot \tau_c \quad (3)$$

Whenever possible, the same calculations were applied to the parameter estimates reported by Massof et al.<sup>7</sup> and Grover et al.,<sup>9</sup> which are the two published studies that most closely approximate the analyses that we performed in this investigation, and to two other published studies.<sup>6,8</sup> In so doing, we sought to compare our estimates to published ones for patients with RP and to determine whether the natural history of visual field loss in Usher syndrome type II mimics that of nonsyndromic RP, or, rather, differs from it in some respect. For all the estimates of our interest (the intercept  $\alpha$ , the slope  $\beta$ , the time constant  $\tau_c$ , and the half-life  $t_{0.5}$ ) we also calculated the 95% confidence interval (CI).

## RESULTS

Figures 1 and 2 illustrate the relationship between visual field area for both the I4e and the V4e targets with age and symptomatic disease duration, respectively. It is immediately evident (1) that virtually all patients experienced some decline in visual field area over time, with either one target or both, consistent with the progressive nature of the retinal degeneration of Usher syndrome, and (2) that, although there was no immediate pattern in the kinetics of visual field loss that was revealed by plotting the area data as a function of age, normalization to symptomatic disease duration shifted most data points along a common curve. Therefore, this descriptive analysis suggested that the kinetics of this phenomenon were better explained by symptomatic disease duration than by chronological age.

The curves described by the data points for the two targets in Figure 2 have some important characteristics. First, areas for the V4e target remained essentially stable up to 10 years of symptomatic disease, whereas the areas of the corresponding I4e targets at the same time points were already deteriorating rapidly. After this initial plateau, also the area of the V4e target began decreasing, with a slope similar to that of the I4e areas. The latter appeared to experience a steady decline since the onset of symptomatic disease, with no initial plateau phase.

After approximately 10 years of symptomatic disease, the rate of decline of the I4e area appeared to diminish in parallel to the simultaneous acceleration of the decline in the V4e area. After 16 to 22 years of symptomatic disease, the rate of decline of the V4e target also decreased, showing a slower decline over the subsequent 25 years of symptomatic disease. Although this end-stage plateau could be partially explained by the I4e target's becoming too small for some patients to detect (therefore, recorded as a zero area), this was not the case for the V4e target, which was still detectable by all subjects and was still experiencing a slower yet persistent decline over the years. This suggested that after the initial plateau for the V4e target, areas for the two targets followed similar kinetics of decline over time and that these kinetics appeared to be exponential in both cases, since disease onset for the I4e target and after the initial plateau for the V4e target.

## Mixed-Model Analysis of the Data

Based on these observations, we fit with the mixed-model procedure the natural log of the visual field areas as a function of age and symptomatic disease duration, respectively. The results of these analyses are summarized in Tables 2 and 3, respectively. Both chronological age and duration of symptomatic disease were significant predictors of visual field decline over time, but symptomatic disease duration offered a significantly better fit of the data than age. When chronological age was used, three intercept estimates and two  $\beta_{\text{age}}$  estimates for the V4e data, and one intercept and one  $\beta_{\text{age}}$  estimate for the I4e data deviating significantly (seven total deviant estimates, all to levels of significance of 0.04 or less, and as low as 0.0007) from the predicted model. Only two estimates deviated when symptomatic disease duration was used.

Baseline age and sex were not related to visual field area ( $P > 0.4$  under all circumstances, not shown) when added to the model containing symptomatic disease duration, nor were there any significant interactions between any of the study variables (not shown). To determine whether the inclusion of subjects for whom only two serial data points were available had affected significantly the fit of the model and the parameter estimates, we repeated the mixed-model analysis eliminating the six subjects for whom only two observations were available. The fit of the model was virtually unchanged (data not shown).

Because the data were well explained by exponential dynamics, we fit the following equation

$$\text{GVF area} = e^{(\alpha - \beta \cdot x_{ij})} \quad (4)$$

where  $x_{ij}$  is the duration of symptomatic disease (in years) at the  $i^{\text{th}}$  observation on the  $j^{\text{th}}$  subject. The parameter estimates for the intercept ( $\alpha$ ) and the slope ( $\beta$ ) obtained with the original analysis (Table 3) for symptomatic disease duration were therefore used to construct the equation predictive of the visual field areas with the I4e and V4e targets.

Based on equation 4, we constructed the best-fit curves for the visual field areas delimited with the two investigated targets—the mean and the confidence interval of which are shown in Figure 2. The models appear to fit the observed data well, although the fit is somewhat closer for the V4e data. Furthermore, from the intersection of the best-fit line with the lowest limit of normal for the two targets of the visual field (dotted lines along the  $y$ -axis in Fig. 2), we empirically determined the intersection with the  $x$ -axis to obtain an estimate of the interval of symptomatic years separating the beginning of the loss in I4e area from that to the V4e target (i.e., the “critical age” of Massof et al.<sup>7</sup>). Based on this extrapolation, the I4e area loss is predicted to begin approximately 7 years before the

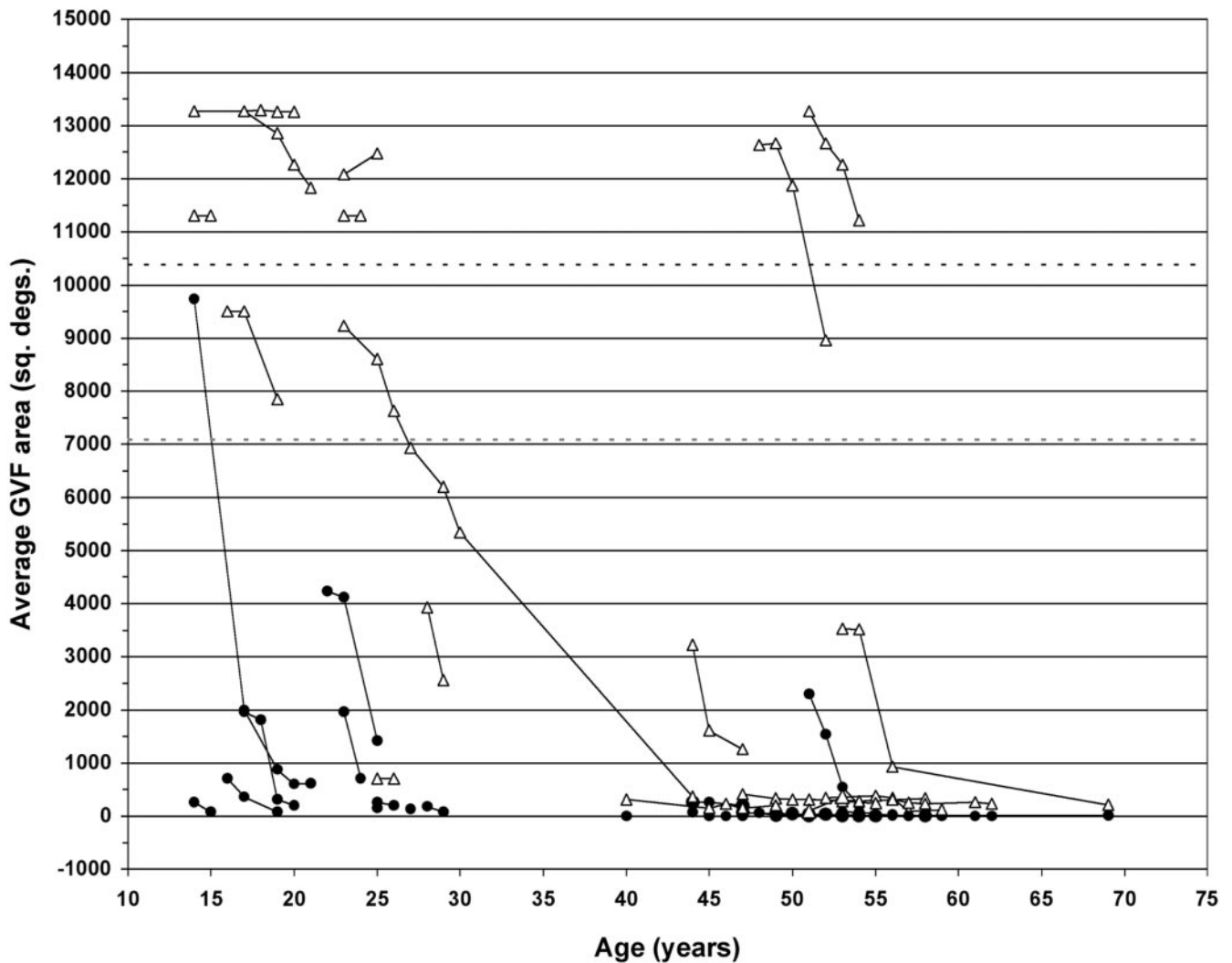


**FIGURE 1.** GVF area as a function of age. ( $\Delta$ ) and ( $\bullet$ ) identify V4e and I4e data, respectively; each set of symbols connected by a continuous line represents data from an individual patient. Dotted horizontal line and dotted gray horizontal line identify the lower limits of normal (5th percentile) of a GVF area for the V4e and the I4e targets, respectively. In numerical terms, this corresponded to 10,381 deg<sup>2</sup> for the V4e target (equivalent to a visual field of 115° in average diameter) and to 7,085 deg<sup>2</sup> for the I4e target (equivalent to a visual field of 95° in average diameter). Larger visual fields tended to exhibit a steeper decline. Some patients, however, were remarkable for visual field preservation in late age (e.g., PT11 and PT16), which was consistent with the late onset of their subjective symptoms.

disease becomes symptomatic—that is, subjectively appreciated by the patient, whereas the area loss to the V4e target is predicted to begin after approximately 8 years of symptomatic disease. The latter observation fits quite well with the observed V4e data, which indeed started to show a measurable decline approximately 6 to 10 years after onset of symptoms in most of the subjects in that area range.

In addition, based on the parameter estimates shown in Table 3 and based on equations 2 and 3,<sup>7,9</sup> we calculated: (1) the time constants for the two targets,  $\tau_{cI4e}$  and  $\tau_{cV4e}$ , which were estimated to be 5.8 years (95% CI: 4.6–7.9) and 7.4 years (95% CI: 6.5–8.6), respectively; and (2) the visual field half-lives,  $t_{0.54e}$  and  $t_{0.5V4e}$ , which were estimated at approximately 4 (95% CI: 3.2–5.5) and 5 (95% CI: 4.5–5.9) years, respectively.

In summary, our analysis estimated that approximately 17.2% of the remaining I4e area (95% CI: 12.7%–21.6%) and 13.6% of the remaining V4e area (95% CI: 11.7%–15.5%) are lost by patients affected with Usher syndrome type II for every year of symptomatic disease and that the loss of approximately 50% of the original remaining area of the visual field can be

expected to occur, on average, in about 4 years of symptomatic disease for the I4e target and 5 years for the V4e target.

The small differences in the estimated slopes, time constants, and half-lives were not statistically significant, as the confidence intervals of one target estimate always included the mean of the estimate obtained for the other target. However, an almost identical difference had been noted before by Massof et al.<sup>7</sup> and had been attributed to the possible ceiling and/or floor effect exerted on the V4e slope by data at either extreme of the curve, making it artificially more shallow. We therefore repeated the analysis after removing data points in the normal range responsible for the initial plateau observed for the V4e target and for the first I4e observation of PT2. This analysis resulted in slope estimates that were more divergent than before (not shown), indicating that the observed differences in the slopes for the I4e and V4e target were not accounted for by the data points excluded in the repeat analysis. Exclusion of the I4e area data points recorded as zero areas (i.e., once this target was no longer detectable by the patients) also failed to modify appreciably the fit of the model (not shown), indicating

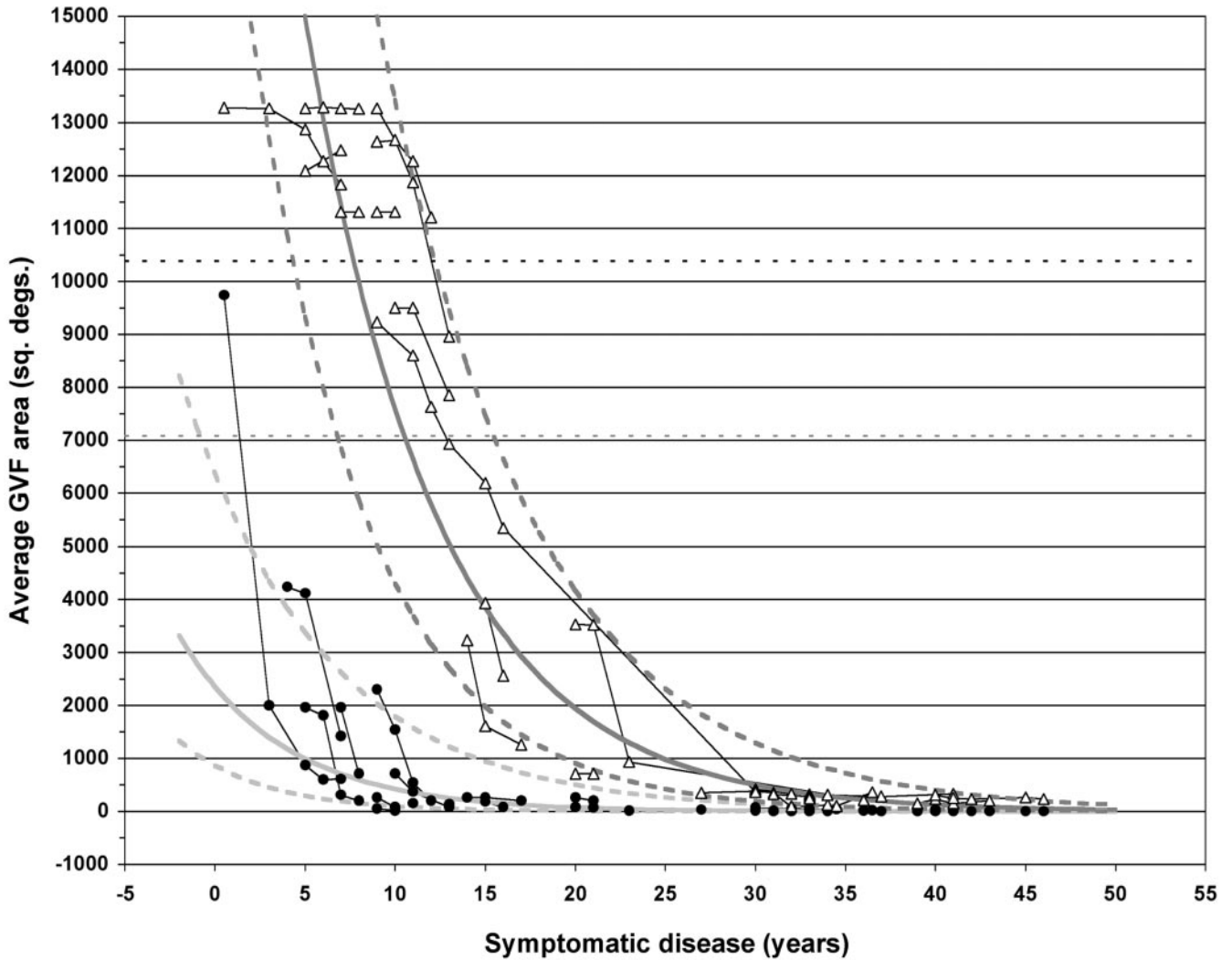


FIGURE 2. GVF area as a function of symptomatic disease duration. Symbols and delineations are as in Figure 1. Normalization of the visual field area data to the estimated symptomatic disease duration, (i.e., years of symptomatic disease after the onset of night blindness) eliminated the data scatter observed in Figure 1. Both the I4e and the V4e data appear to cluster nicely together: the former after an exponential decay since disease onset, the latter after approximately the same decay kinetics but after an initial plateau phase. The solid and dashed dark gray curves represent the predicted best-fit line and the 95% CI around this estimate derived from application of equation 4 to the result of the mixed-model analysis of the V4e data. The solid and dashed light gray curves represent the best-fit line and the 95% CI around this estimate for the I4e data.

that the slope estimate for the I4e target was not driven by a floor effect exerted by the end-stage disease data.

**Estimated Yearly Rates of Visual Field Loss**

The characterization of the kinetics of visual field loss in Usher syndrome type II offers us the ability to attempt a more accurate prognostic judgment for patients with this disease. Specifically, the establishment of the age of onset of the first symp-

toms of the disease allows us to formulate more precise predictions, independent of the chronological age of the patient. Based on our estimates obtained in this cohort of patients, it appears that individuals with Usher syndrome type II are bound to experience an average loss of the remaining visual field of 17.2% per year with the I4e standard target and of 13.6% with the V4e target, regardless of gender or age of onset. The estimates based on ln-transformed data that we illustrated

TABLE 2. Parameter Estimates and Statistics (Solution for Fixed Effects) for Age as the Independent Variable in the Model Based on Mixed-Model Regression

Dependent Variable	Estimate	SE	95% CI	t	P
ln(area) I4e					
Intercept ( $\alpha$ )	9.160	0.905	7.386 to 10.933	10.12	<0.0001
Slope ( $\beta_{age}$ )	-0.125	0.026	-0.176 to -0.075	-4.87	<0.0001
ln(area) V4e					
Intercept ( $\alpha$ )	10.904	0.775	9.385 to 12.424	14.06	<0.0001
Slope ( $\beta_{age}$ )	-0.084	0.017	-0.118 to -0.050	-4.88	0.0001

**TABLE 3.** Parameter Estimates and Statistics (Solution for Fixed Effects) for Symptomatic Disease Duration as the Independent Variable in the Model

Dependent Variable	Estimate	SE	95% CI	<i>t</i>	<i>P</i>
ln(area) I4e					
Intercept ( $\alpha$ )	7.765	0.508	6.768 to 8.761	15.27	<0.0001
Slope ( $\beta_{\text{disdur}}$ )	-0.172	0.023	-0.216 to -0.127	-7.53	<0.0001
ln(area) V4e					
Intercept ( $\alpha$ )	10.296	0.193	9.917 to 10.675	53.28	<0.0001
Slope ( $\beta_{\text{disdur}}$ )	-0.136	0.010	-0.155 to -0.117	-13.97	<0.0001

in the previous paragraphs can be converted in readily applicable numerical values, and the actual yearly rate of visual field loss can be estimated as follows

$$\text{Area loss} = 1 - e^{(-\beta \cdot x_{ij})} \quad (5)$$

where  $x_{ij}$  is the same as in equation 4. The predicted average area loss over a number of representative years of symptomatic disease is shown in Table 4. These values are intended to represent areas below the lower limit of normal. Therefore, although the observed values demonstrated that some degree of loss can occur for the V4e target even while values still fall within normal limits, it is assumed for simplicity that no detectable loss could be measured until the lower limit of normal of the V4e area was crossed (i.e., according to our estimate, after 8 years of symptomatic disease).

## DISCUSSION

We characterized the kinetics of visual field loss in a longitudinal cohort of 19 patients affected with Usher syndrome type II. The results of this analysis indicate that the extent of decline in GVF area that is predicted to occur in this progressive degenerative retinal disorder was better correlated with the duration of symptomatic disease since the onset of night blindness, than by chronological age.

Findings in earlier studies<sup>6-9</sup> and in ours are summarized for comparison purposes in Table 5. Although our estimates suggest that patients with Usher syndrome type II may have faster disease progression rates than the average RP patient, this difference was not statistically significant. In fact, taking into account the confidence interval for each study, our findings appear fairly consistent with most previous investigations. Our results are especially consistent with those of Massof et al.,<sup>7</sup> who also noted that the kinetics of visual field decay in patients with RP were exponential and remarkably similar among patients and among genetic subgroups, once the time-dependent variable was normalized to the critical age—that is, the extrapolated age after which the exponential decay would begin. Even more remarkable is the similarity of the slopes, the time constant ( $\tau_c$ ), of the decay of visual field and, consequently, of the half-life ( $t_{0.5}$ ) of the visual field areas from our investigation with those that Massof et al.<sup>7</sup> estimated. This was true even for the comparison between target I4e in our study and II4e in theirs, although this comparison is somewhat spurious because the latter target is four times as large as the standard I4e (1 mm<sup>2</sup> vs. 0.25 mm<sup>2</sup>). The results in the study by Berson et al.<sup>6</sup> appear to be the least consistent compared with both our study and the others, a discrepancy noted also by Grover et al.<sup>9</sup> However, Berson et al. averaged the V4e visual field area of all study participants at baseline, and compared it with the average areas at one, 2 and 3 years of follow-up. This analysis strategy is quite

**TABLE 4.** Predicted Visual Field Area Loss as a Function of Symptomatic Disease Duration

Symptomatic Disease (y)	I4e Target		V4e Target	
	Average Area Loss*	95% CI	Average Area Loss*	95% CI
1	0.747	0.638-0.822	N/O	—
2	0.787	0.681-0.857	N/O	—
3	0.821	0.719-0.885	N/O	—
4	0.849	0.753-0.907	N/O	—
5	0.873	0.782-0.925	N/O	—
6	0.893	0.808-0.940	N/O	—
7	0.910	0.831-0.951	N/O	—
8	0.924	0.851-0.961	N/O	—
9	0.936	0.869-0.968	0.127	0.110-0.144
10	0.946	0.885-0.975	0.238	0.209-0.267
12	0.962	0.910-0.983	0.420	0.374-0.462
14	0.973	0.931-0.989	0.558	0.504-0.605
16	0.981	0.946-0.993	0.663	0.608-0.711
18	0.986	0.958-0.995	0.743	0.690-0.788
20	0.990	0.968-0.997	0.804	0.754-0.844
25	0.996	0.983-0.999	0.901	0.863-0.928
30	0.998	0.991-1.000	0.950	0.924-0.967
35	0.999	0.995-1.000	0.975	0.958-0.985
40	1.000	0.997-1.000	0.987	0.976-0.993

Data are based on slope estimates (I4e: -0.172; V4e: -0.136) and extrapolated "critical ages" (I4e: 7 years prior to onset; V4e: 8 years after symptom onset). N/O, not observed.

\* Fraction of the original area below the lowest normal limit.

TABLE 5. Summary of Findings from Published Studies on the Natural History of Goldmann Visual Field Decline Over Time in RP Versus the Present Study

Author Target (Sample Size)	Mean Slope ( $\beta$ ) (Range* or CI†)	Time Constant ( $\tau_c$ ) (Range* or CI†)	Half-Life ( $t_{0.5}$ ) (Range* or CI†)
Berson et al. <sup>6</sup> V4e (n = 90)	-0.046 (N/A)	21.74 (N/A)	15.07 (N/A)
Massof et al. <sup>7</sup> II4e (n = 172)‡	-0.170 (N/A)	7.40 (6.64 to 8.17)†	5.13 (4.60 to 5.66)†
V4e (n = 172)§	-0.145 (N/A)	8.40 (7.63 to 9.17)†	5.82 (5.29 to 6.36)†
Holopigian et al. <sup>8</sup> V4e (n = 23)¶	-0.112 (-0.192 to -0.032)†	8.95 (6.78 to 12.63)†	6.20 (4.70 to 8.75)†
Grover et al. <sup>9</sup> II4e (n = 71)	-0.102 (-0.116 to -0.078)*	9.81 (8.57 to 12.84)*	6.80 (4.80 to 9.50)*
V4e (n = 77)	-0.095 (-0.144 to -0.073)*	10.53 (6.93 to 13.71)*	7.30 (6.00 to 8.90)*
Present study I4e (n = 19)	-0.172 (-0.216 to -0.127)†	5.83 (4.63 to 7.89)†	4.04 (3.21 to 5.47)†
V4e (n = 19)	-0.136 (-0.155 to -0.117)†	7.35 (6.45 to 8.55)†	5.07 (4.47 to 5.93)†

\* The reported ranges refer to analyses conducted either by subgroup or by year.

† CI, 95% confidence interval (as reported or calculated).

‡ The mean slope was calculated with  $n = 645$ , the other variables with  $n = 145$ .

§ The mean slope was calculated with  $n = 720$ , the other variables with  $n = 157$ .

¶ Data derived from the half-life ( $t_{0.5}$ ) estimate and associated standard deviation reported in the original manuscript.

different from the more recently developed mixed-model procedure that Massof et al.,<sup>7</sup> Grover et al.,<sup>9</sup> and we were able to use. Therefore, it is possible that this difference in analytical approach explains the apparent inconsistency.

Our study is the first to focus on Usher syndrome type II. Berson et al.<sup>6</sup> explicitly excluded syndromic cases in their study, whereas Holopigian et al.<sup>8</sup> had only one such patient in their cohort. Grover et al.<sup>9</sup> included in their study data on 24 patients with Usher syndrome type II for the V4e area and on 16 for the II4e area, but did not perform any subgroup analysis by disease type, nor did they use symptomatic disease duration or critical age as a criterion to normalize their data. Therefore, we are unable to compare our findings with theirs fully. Last, Massof et al.,<sup>7</sup> whose data-analysis strategy and outcomes are perhaps the closest to ours, did not comment specifically on whether patients with Usher syndrome were included in their study, nor did they present data on them as a separate subgroup. Therefore, it appears reasonable to state that our study confirms that the exponential decay model proposed by Massof et al.<sup>7</sup> describes well the deterioration of visual fields in hereditary retinal degenerations over time, and specifically extends this finding to Usher syndrome type II. Whether the rates of visual field decline observed in our study are generalizable to all patients with Usher syndrome type II remains to be verified.

Our results suggest that, regardless of genetic heterogeneity, patients with rod  $\geq$  cone retinal dystrophy may experience a decline in their visual fields according to the same kinetics. Consequently, consistent with what was first hypothesized by Massof et al.,<sup>7</sup> our findings suggest the existence of stereotypical disease mechanism(s) that may characterize most patients with RP and related conditions once their degenerative process has become symptomatic. A consequence of this conclusion is that genetic and allelic heterogeneity in hereditary retinal degenerations, at least of the rod  $\geq$  cone type, would appear to be mainly responsible for differences in the age of onset of the

symptoms across genetic subtypes and to some extent in rates of disease progression, but that once the disease process has begun, its kinetics are virtually the same from a mechanistic point of view for most patients.

The concept of symptomatic disease duration that we propose here is similar to that of critical age proposed by Massof et al.,<sup>7</sup> the main difference being that our variable was ascertained directly from the individual patient and not extrapolated from the analysis of a large data set. Massof et al. also observed in their study that critical age correlated closely with another symptom, the onset of subjective appreciation of visual field loss. It has been reported before that the latter typically occurs later than the onset of night blindness in all types of RP in general, and specifically in Usher syndrome type II,<sup>27</sup> and this was verified in the present study. This finding demonstrates that the ascertainment of disease onset by careful questioning in the clinical setting can be used as a reliable and meaningful criterion to predict the ensuing disease kinetics in patients with Usher syndrome type II.

Although the generalizability of our findings with respect to symptomatic disease duration may be limited by the relatively small sample size ( $n = 19$ ), the homology between our findings and those of Massof et al.<sup>7</sup> is remarkable and raises the possibility that this readily obtainable piece of information may be used equally reliably and effectively in RP in general. Likewise, it is not known whether our findings about the kinetics and slope estimates for this cohort could be generalized to all patients with Usher syndrome type II. The reason(s) why certain patients do not have symptoms of retinal disease well into the fourth or fifth decade of life also remains unknown. Instances of late-onset RP in congenitally hearing-impaired patients harboring *USH2A* mutations have been reported previously.<sup>5</sup> "Weak" recessive alleles, compromising only mildly the function of the encoded protein in the retina, may be the simplest explanation. Alternatively, although mutations in *USH2A* are responsible for most cases of Usher syndrome type

II<sup>28,29</sup> and it is therefore unlikely that our study patients included a significant number of cases other than Usher syndrome type IIa, the late-onset cases in our cohort may represent a genetically separate subset. Also, other genetic and epigenetic modifiers may be responsible for these late-onset phenotypes. Their identification could be of paramount importance to devising therapeutic strategies for Usher syndrome type II other than gene therapy.<sup>30</sup> Two important corollaries to this observation are that (1) because retinal degeneration appears to follow the same exponential kinetics in the late-onset phenotypes, these putative modifiers may exert an effect on age of onset but not (or less) on disease kinetics, once triggered; and that (2) the diagnosis of Usher syndrome type II may not be excluded in patients born with partial hearing loss, even if a functional work-up turned out to be normal in childhood, and possibly as late as in the fourth decade of life. In the future, it would be interesting to extend this type of analysis to a larger data set and examine how mutations in different *USH2* genes, or types of mutations (e.g., missense versus nonsense) within one gene, compare with one another as it relates to age of onset.

In summary, our study characterized in detail the kinetics of visual field decay in Usher syndrome type II and identified important similarities between this condition and nonsyndromic RP that suggest the existence of stereotyped decay kinetics once the disease becomes symptomatic. As the chance for forthcoming treatment trials of hereditary retinal degenerations in general, and Usher syndrome in particular, increases with our growing understanding of these conditions, knowledge of the kinetics of the decay of visual function is necessary to be able to make sensible predictions of the achievable therapeutic effect, which are needed to make adequate sample size calculations. Our data indicate that failure to stratify the allocation of patients to different treatment trial arms according to visual-field-related disease-staging criteria may bias the interpretation of such trials, thereby jeopardizing their outcome. The continued refinement of our understanding of the natural history of visual function variables in patients with hereditary retinal degenerations will allow us to create the indispensable premises to the performance of additional scientifically sound and rational randomized treatment trials for these conditions.

## References

- Pagon RA. Retinitis pigmentosa. *Surv Ophthalmol.* 1988;33:137-177.
- Fishman GA, Kumar A, Joseph ME, Torok N, Anderson RJ. Usher's syndrome: ophthalmic and neuro-otologic findings suggesting genetic heterogeneity. *Arch Ophthalmol.* 1983;101:1367-1374.
- Smith RJH, Berlin CI, Hejtmancik JF, et al. Clinical diagnosis of the Usher syndromes. Usher Syndrome Consortium. *Am J Med Genet.* 1994;50:32-38.
- Iannaccone A. Usher syndrome: correlation between visual field size and maximal ERG response b-wave amplitude. In: *Retinal Degenerations: Mechanisms and Experimental Therapy.* LaVail MM, Hollyfield JG, Anderson RE, eds. New York: Plenum Publishers; 2003:123-131.
- Liu XZ, Hope C, Liang CY, et al. A mutation (2314delG) in the Usher syndrome type IIA gene: high prevalence and phenotypic variation. *Am J Hum Genet.* 1999;64:1221-1225.
- Berson EL, Sandberg MA, Rosner B, Birch DG, Hanson AH. Natural course of retinitis pigmentosa over a three-year interval. *Am J Ophthalmol.* 1985;99:240-251.
- Massof RW, Dagnelie G, Beneschawel T, Palmer RW, Finkelstein D. First-order dynamics of visual field loss in retinitis pigmentosa. *Clin Vis Sci.* 1990;5:1-26.
- Holopigian K, Greenstein V, Seiple W, Carr R. Rates of change differ among measures of visual function in patients with retinitis pigmentosa. *Ophthalmology.* 1996;103:398-405.
- Grover S, Fishman GA, Anderson RJ, Alexander KR, Derlacki DJ. Rate of visual field loss in retinitis pigmentosa. *Ophthalmology.* 1997;104:460-465.
- Grover S, Fishman GA, Brown J Jr. Patterns of visual field progression in patients with retinitis pigmentosa. *Ophthalmology.* 1998;105:1069-1075.
- Birch DG, Anderson JL, Fish GE. Yearly rates of rod and cone functional loss in retinitis pigmentosa and cone-rod dystrophy. *Ophthalmology.* 1999;106:258-268.
- Grover S, Fishman GA, Anderson RJ, Lindeman M. A longitudinal study of visual function in carriers of X-linked recessive retinitis pigmentosa. *Ophthalmology.* 2000;107:386-396.
- Rivolta C, Sweklo EA, Berson EL, Dryja TP. Missense mutation in the *USH2A* gene: association with recessive retinitis pigmentosa without hearing loss. *Am J Hum Genet.* 2000;66:1975-1978.
- Iannaccone A, Vingolo EM, Rispoli E, et al. Electroretinographic alterations in the Laurence-Moon-Bardet-Biedl phenotype. *Acta Ophthalmol Scand.* 1996;74:8-13.
- Iannaccone A, Rispoli E, Vingolo EM, et al. Correlation between Goldmann perimetry and maximal electroretinogram response in retinitis pigmentosa. *Doc Ophthalmol.* 1995;90:129-142.
- Sandberg MA, Weigel-DiFranco C, Rosner B, Berson EL. The relationship between visual field size and electroretinogram amplitude in retinitis pigmentosa. *Invest Ophthalmol Vis Sci.* 1996;37:1693-1698.
- Piazza L, Fishman GA, Farber M, Derlacki D, Anderson RJ. Visual acuity loss in patients with Usher's syndrome. *Arch Ophthalmol.* 1986;104:1336-1339.
- Fishman GA, Anderson RJ, Lam BL, Derlacki DJ. Prevalence of foveal lesions in type 1 and type 2 Usher's syndrome. *Arch Ophthalmol.* 1995;113:770-773.
- Edwards A, Fishman GA, Anderson RJ, Grover S, Derlacki DJ. Visual acuity and visual field impairment in Usher syndrome. *Arch Ophthalmol.* 1998;116:165-168.
- Berson EL, Rosner B, Sandberg MA, et al. A randomized trial of vitamin A and vitamin E supplementation for retinitis pigmentosa. *Arch Ophthalmol.* 1993;111:761-772.
- Szyk JP, Alexander KR, Severing K, Fishman GA. Assessment of driving performance in patients with retinitis pigmentosa. *Arch Ophthalmol.* 1992;110:1709-1713.
- Ross DF, Fishman GA, Gilbert LD, Anderson RJ. Variability of visual field measurements in normal subjects and patients with retinitis pigmentosa. *Arch Ophthalmol.* 1984;102:1004-1010.
- Sunga RN, Sloan LL. Pigmentary degeneration of the retina: early diagnosis and natural history. *Invest Ophthalmol.* 1967;6:309-325.
- Dagnelie G. Conversion of planimetric visual field data into solid angles and retinal areas. *Clin Vision Sci.* 1990;5:95-100.
- Massof RW, Finkelstein D, Starr SJ, et al. Bilateral symmetry of vision disorders in typical retinitis pigmentosa. *Br J Ophthalmol.* 1979;63:90-96.
- Littell RC, Milliken GA, Stroup WW, Wolfinger RD. Random coefficient models. In: *SAS System for Mixed Models.* Cary, NC: SAS Institute Inc.; 1996:253-266.
- Heckenlively JR, Yoser SL, Friedman LH, Oversier JJ. Clinical findings and common symptoms in retinitis pigmentosa. *Am J Ophthalmol.* 1988;105:504-511.
- Leroy BP, Aragon-Martin JA, Weston MD, et al. Spectrum of mutations in *USH2A* in British patients with Usher syndrome type II. *Exp Eye Res.* 2001;72:503-509.
- Najera C, Beneyto M, Blanca J, et al. Mutations in myosin VIIA (*MYO7A*) and usherin (*USH2A*) in Spanish patients with Usher syndrome types I and II, respectively. *Hum Mutat.* 2002;20:76-77.
- Bhattacharya S. Gene therapy: when, and for what? *The Lancet.* 1995;345:739-740.